

present examples of these plots. Included on the plots are the points and fixes specified by the siting engineer. In addition, probability of detection (P_D) and probability of false alarm (P_{FA}) performance plots can also be generated in a number of user-selectable formats. An example range-azimuth format performance plot is illustrated in Fig. 4, while an example range-height format performance plot is illustrated in Fig. 5. The P_D and other performance values can also be determined for a user-specified aircraft flight path.

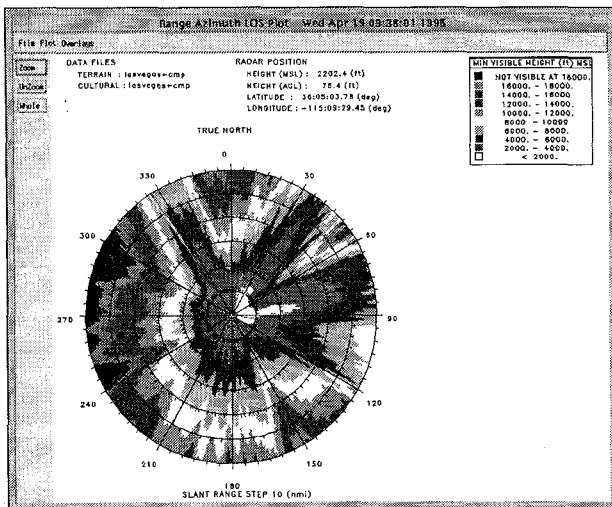


Fig. 2. LOS Visibility Plot

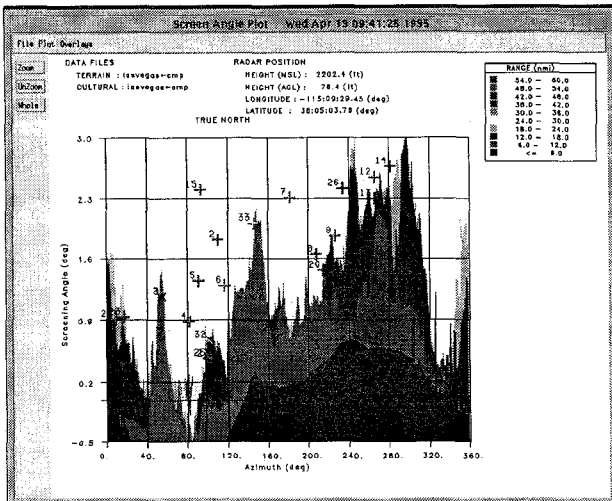


Fig. 3. Obscuration Angle Plot

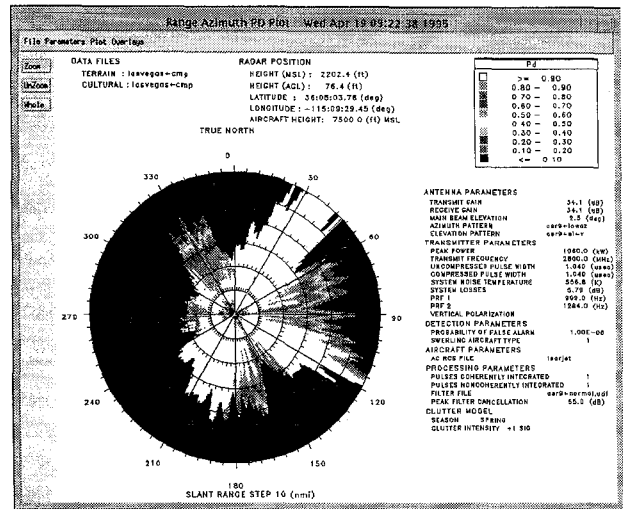


Fig. 4. Probability of Detection Plot in Range-Azimuth Format

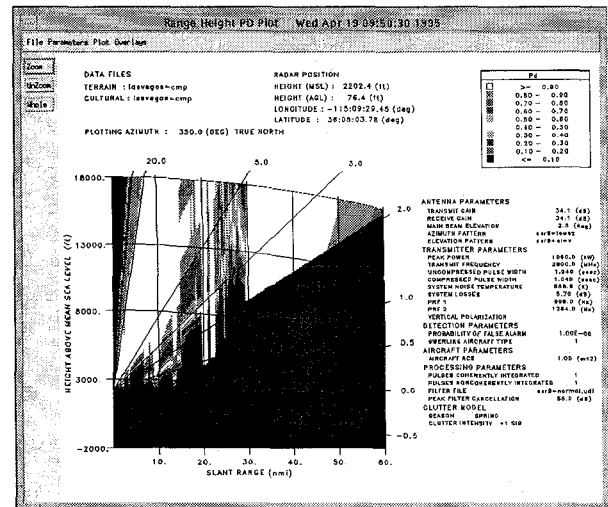


Fig. 5. Probability of Detection Plot in Range-Height Format

SSR performance is also available in a variety of output formats. For example, this data can be presented as the received signal-to-noise ratio (SNR) for the interrogator or the transponder, as the probability of correctly receiving a message on the uplink or the downlink path, or as the round-reliability of the entire system. Also available are plots of probable false beacon reply locations; such false replies are due to reflections from buildings and other structures.

Two validations of the clutter/LOS modeling have been performed. The first was performed by the MITRE Corporation, using data collected with an X-band radar at the Miramar Naval Air Station in California. The second validation was performed by Technology Service Corporation with the cooperation and support of Rome Laboratory, using the S-band radar located at their Rome, NY facility. Both comparisons showed that the LOS and clutter RCS processing of

the RSS to be performing well within expected bounds. A third validation using an instrumented ASR-9 radar in Albuquerque, NM will be performed in 1997. Also during 1997 a validation of the ARSR-4 model will be performed.

The RSS has been used to support a number of sensor siting and analysis projects. For example, the RSS was used to assist in the siting of both PSRs and SSRs in Tunisia, and to provided performance data to the FAA's Central Region to aid in the justification of an ASR-9 radar site selection. Additionally, the RSS is currently being used by the FAA as a system evaluation tool, performing analyses of proposed sensor designs and hardware modifications in simulated site-specific environments. A variant of the RSS, known as the FIREFINDER Position Analysis System (FFPAS), has been developed for the US Army. The FFPAS is presently being used by the Army to site counter-battery radars in Bosnia and South Korea.

II. RSS OPERATION

The RSS, which operates under UNIX, has been developed using X-Windows and Motif. The software is coded in C and FORTRAN. At the present stage of its development the RSS models the performance of L-band through K_u -band PSRs. Fig. 6 illustrates the basic processing stages for an RSS radar performance analysis. Each stage of the processing will be discussed in the following subsections.

A. User Interface

The user interface to the RSS is through a menu-driven program from which the engineer can specify the parameters of the sensor system to be analyzed, detail the site-specific characteristics, and select from a set of output formats. The menu system allows the user the flexibility of performing analyses utilizing stored sensor parameter files, generating variations on the stored files, or creating additional parameter files describing new or developmental radar systems. Fig. 7 presents an RSS menu example. This particular menu is used to input the parameters for the sensor's transmit antenna.

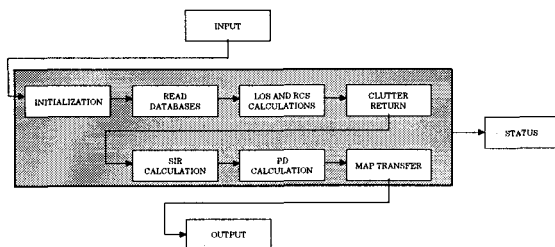


Fig. 6. RSS Processing Stages

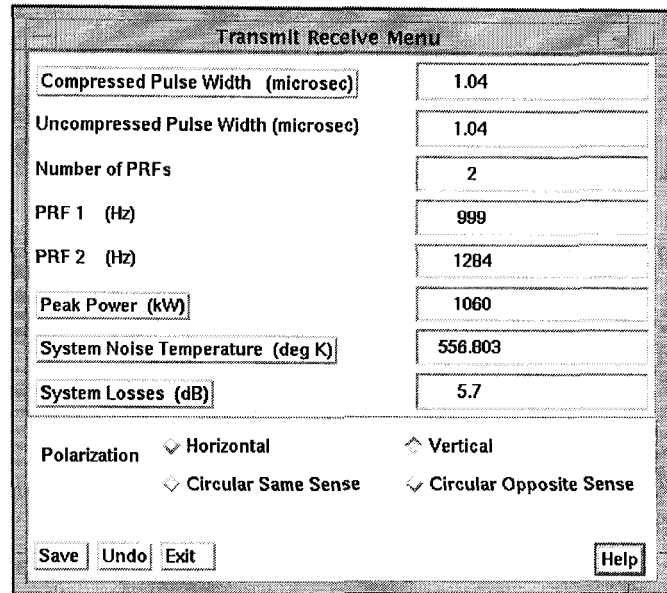


Fig. 7. RSS Menu Example

B. Databases

Three databases are used in the current version of the RSS to describe the local environment of the sensor. The first, illustrated in Fig. 8, is a Digital Elevation Model (DEM) that describes the topography of the locale. The DEM consists of a latitude/longitude grid of terrain elevations. The height resolution of this database is one meter, with steps in latitude and longitude of three seconds. This database is available from the United States Geological Survey (USGS) or from the Defense Mapping Agency (DMA).

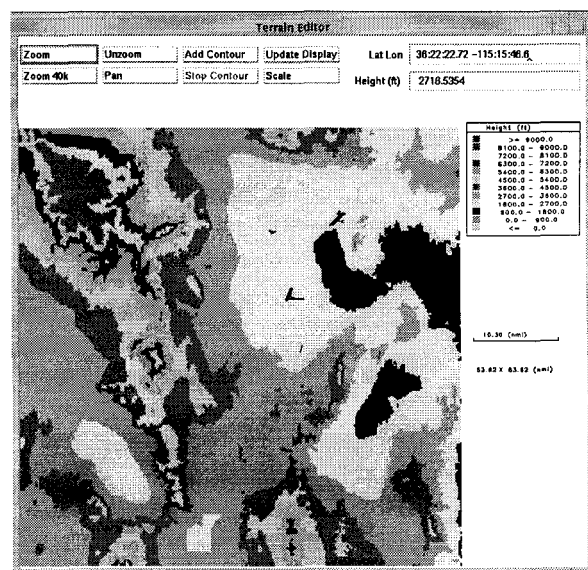


Fig. 8. Digital Terrain Height Database

The second required database, illustrated in Fig. 9, is the Land Use and Land Cover (LULC) model, which can also be purchased from the USGS. This database consists of a latitude/longitude grid of selected terrain cover types. The latitude and longitude resolution of the LULC database is also three seconds. For an ASR-9 analysis, the terrain height and the terrain cover databases typically encompass a 120 nmi square area centered at the airport. Significantly larger databases are required for an enroute system such as the ARSR-4.

The third database, which is optional but which is very important for urban sitings, is termed the cultural database. This database, illustrated in Fig. 10, is a collection of three-dimensional models of all of the significant buildings in the proximity of the airport. Each building is represented as a polygon, with each vertex of the polygon being defined by its latitude and longitude, the ground height (MSL) at the base and the height (MSL) of that point above the base. Also included is an estimate of the construction material of each structure. All buildings with a vertical projected area greater than 100 m² within 10 nmi of the airport are currently collected. The cultural database is typically collected from 1:40,000 aerial stereo photographs of the area using a specialized digital stereoplotter.

Another part of the RSS tool set is an interactive, graphics-based cultural database editor. This editor allows the analyst to permanently modify the cultural database to incorporate new construction in the vicinity of the airport. The editor also permits the analyst to make temporary changes in the cultural database, allowing, for example, the impact of proposed construction on existing radar sites to be determined.

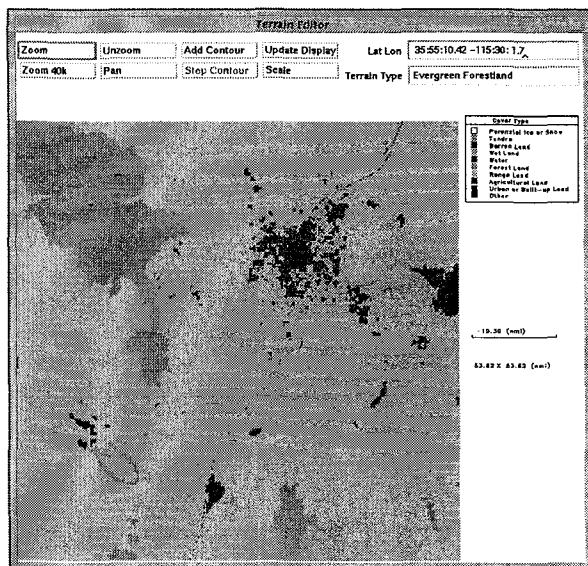


Fig. 9. Digital Terrain Cover Database

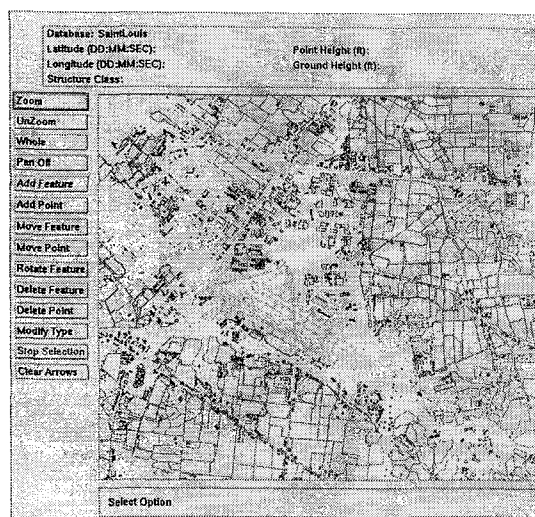


Fig. 10. Cultural Database

C. LOS Visibility Determination and Clutter Cancellation Processes

The LOS visibility determination and clutter calculation processes can be logically separated into the five stages shown in Fig. 6. (To minimize computational complexity and data storage requirements, some of these stages are intertwined.) In the first stage, the terrain databases are organized in a range/azimuth format, with an increasingly fine azimuth resolution as the range from the sensor location increases. This is done to ensure a minimum cross-range resolution, which is currently set to 100 m.

In the second stage, the RCS of all visible terrain cells is calculated using one of two parametric terrain backscatter models that have been chosen for use in the RSS. The first model, which is used at UHF, was formulated by the Air Force; the second model, which is used for L through X-bands, was developed by Ulaby and Dobson. Both models are valid for all incidence angles, ψ . The clutter reflectivity, σ_o , predicted by these models is:

$$\text{UHF: } \sigma_o = C_1 + \gamma \sin(\psi) + C_2 \exp[-C_3 / (\pi/2 - \psi)]^{C_4} \quad \text{m}^2/\text{m}^2$$

and

$$\text{L to X-band: } \sigma_o = P_1 + P_2 \exp(-P_3 \psi) + P_4 \cos(P_5 \psi + P_6) \quad \text{dBm}^2/\text{m}^2$$

The constants in these models are the terrain, season, polarization and frequency-dependent constants. The expressions are attractive because they allow independent calculation of the constants from separate sets of independent data points.

Model parameters have been determined empirically, based upon measurements of clutter RCS at UHF through X-

band, for various terrain types at grazing angles ranging from near zero degrees to vertical incidence. For K_u -band radar modeling, the σ_0 values have been estimated by extrapolation in frequency to support the ASDE-3 analyses.

The processing of the cultural database begins in Stage 3. Each building in the database is divided into a number of rough plate and dihedral surfaces. The RCS of each plate is calculated based on its visible area, the construction material, and the incident angle to the sensor, using a rough dielectric plate model. The RCS of each dihedral (which are composed to two plates connected at one vertical edge) is calculated based on the visible area of the composite plates, the construction material, the incidence angle for the sensor, and the dihedral angle between the plates. The LOS blockage of the individual plates and of the terrain behind each object is determined using geometrical optics.

The generation of the clutter maps is completed in Stage 4. (Separate maps are maintained for cultural and terrain clutter so that in later stages of RSS processing, the correct Doppler filter response can be determined). Each range-azimuth cell of the terrain and cultural RCS maps is multiplied by the corresponding transmit and receive antenna gains. The elevation gain is determined by the elevation angle from the sensor to the center of the terrain cell or cultural object. To determine the effect of azimuth sidelobes, the radar's azimuth antenna pattern is circularly convolved with each range ring of each clutter map. The resultant terrain and cultural RCS maps are re-sampled to the range resolution of the sensor being modeled, and are passed on to later stages of processing.

D. Signal-to-Interference Ratio Calculation

The Signal-to-Interference Ratio (SIR) routine calculates the SIR for a range/azimuth grid at a user-specified elevation, or a range/elevation grid for a user-specified azimuth. This is done using the radar range equation. Several moving target indicator (MTI) filtering options are available to the RSS user. The filter response to the actual terrain and cultural clutter, including antenna scanning effects, and to rain (if desired) is calculated. The filter options include delay-line cancellers, weighted Fourier transforms with any number of filters excised about zero frequency (i.e. DC), and user-defined digital filters, which can be used with either a single or dual PRF.

E. Probability of Detection Calculation

Calculating the Probability of Detection (P_D) from the SIR generated in the previous stage is done using the standard formulations. Based on the SIR, the desired Probability of False Alarm (P_{FA}), the Swerling target model, the CFAR loss for the local clutter type and the number of processor outputs to be non-coherently integrated, the estimated P_D is calcu-

lated for each cell. Because the calculation can be very complex, a lookup table of SIR versus P_D is generated. This is done in steps of 1% P_D . This procedure allows for rapid conversion of SIR to P_D over the many cells for which this calculation is desired.

F. Output Processing

The final step of a radar siting analysis is the generation of outputs. Two output devices are currently supported by the RSS: an X-window/PHIGS format monitor and a Hewlett Packard color ink jet printer

A significant variety of outputs are currently available in the RSS for both PSRs and SSRs. These outputs include:

- Terrain Contour Maps
- Range/Azimuth LOS Plots
- Range/Azimuth Clutter Plots
- Range/Azimuth Performance Plots
- Range/Height Performance Plots
- Plan view Performance Plots of Flight Corridors
- Range/Azimuth False Alarm Plots
- Obscuration (i.e. Screening) Angle versus Range Plots
- Beacon False Target Detection Plots

III. ASR-9 OPTIMIZATION

Software incorporated into the RSS allows the user to optimize several of the Variable Site Parameters (VSPs) available in the ASR-9. For this, the user specifies a range of antenna tilt angles to be evaluated; then, for each tilt angle, both the STC and the High Beam/Low Beam window parameters are optimized by the RSS. The STC optimization attempts to maintain an 80% P_D over the desired detection volume, while the High Beam/Low Beam settings are selected to minimize the number of receiver saturations. Weighted performance measures, including the number of remaining receiver saturations, the point/fix visibility and the detection performance are then used to select an optimal tilt angle. Table I presents an example of a point/fix visibility analysis, while Table II shows an example of an optimized VSP determination.

IV. FUTURE RSS ENHANCEMENTS

Many enhancements are being considered by the FAA and AFRL for incorporation into the RSS. These include the modeling of additional sensors such as the Terminal Doppler Weather Radar (TDWR), Parallel Runway Monitors, the ASR-8, ASR-11 and AN/TPS-75 radars, and of enroute communications equipment. The primary planned improvement to the siting software is the capability to auto-

TABLE II
POINT/FIX VISIBILITY ANALYSIS

RADAR LOCATION DATA :											
LATITUDE (DEC MIN SEC)	LONGITUDE (DEC MIN SEC)	ELEVATION (FT MSL)	ANTENNA HT (FT)								
36 05 04	-115 03 26	2195.9	76.4								
FIX DATA :											
NO.	NAME	LATITUDE (DEC MIN SEC)	LONGITUDE (DEC MIN SEC)	RNC (NM)	AZ (DEG-TRUE)	SCREEN ANGLE (DEC)	REQ ALT (FT MSL)	ADJ ALT (FT MSL)	SCREEN VISIBLE	PD	
1	LAS VOR	36 04 47	-115 09 35	0.31	202.89	-1.517	2440.0	****IN BEAM ZONE****		0.000	
2	RD VOR	35 59 45	-114 51 49	15.26	110.29	0.575	3200.0	5171.1	3442.6	YES	0.992
3	OXTO	36 27 30	-114 30 29	36.76	34.24	1.405	8000.0	7572.3	8971.3	NO	X 0.000
4	MEMS	36 09 49	-114 25 30	32.72	81.46	-0.207	8000.0	5723.0	3186.1	YES	X 0.970
5	CRME	36 04 26	-114 13 55	40.16	92.85	0.259	8000.0	8520.8	4820.5	YES	X 0.943
6	WINDS	35 51 23	-114 29 56	36.45	116.49	0.455	7000.0	6742.5	4280.4	YES	X 0.982
7	CRSO	35 46 27	-115 03 55	18.82	191.18	0.838	7000.0	6845.0	4679.7	YES	X 0.993
8	WHLOC	35 30 29	-115 31 25	38.32	207.48	1.193	10000.0	9671.6	7901.6	YES	X 0.995
9	CLMBL	35 40 33	-115 40 47	35.36	226.78	1.507	10000.0	9701.9	8975.9	YES	X 0.972
10	OASIS	35 54 15	-115 23 12	15.58	226.03	1.298	7400.0	7259.1	4494.5	YES	X 0.989
11	WAPLS	36 01 42	-115 22 44	10.85	264.54	1.351	6000.0	5085.7	3636.0	YES	X 0.982
12	LUCKY	36 02 20	-115 50 42	33.61	245.53	2.101	12000.0	11717.6	10432.6	YES	X 0.976
13	WSDN	36 01 42	-115 08 37	41.68	265.43	2.115	12000.0	13145.9	12025.6	YES	X 0.945
14	FUZZY	36 12 02	-115 54 01	36.83	281.13	2.452	12500.0	12191.1	12272.7	YES	X 0.985
15	WAWMO	36 04 35	-114 57 15	9.80	31.75	-0.415	4900.0	4716.5	1677.3	YES	X 0.992
16	LAS 073/2.7	36 04 35	-115 06 51	2.15	103.03	-0.862	2200.0	2181.8	2022.2	YES	X 0.881
17	LAS ARPT	36 04 58	-115 09 13	0.21	118.12	-2.418	2415.0	****IN BEAM ZONE****		0.900	
18	KSNV ARPT	36 14 41	-115 01 27	11.50	33.93	-0.348	2154.0	2055.8	1657.8	YES	X 0.758
19	VOT ARPT	36 12 45	-115 11 46	7.90	945.22	-0.058	2507.0	2440.1	2190.7	YES	X 0.922

* INDICATES PRIMARY FIX

X INDICATES FREE SPACE PD (BEYOND MAX PLUT RANGE)

TABLE III
OPTIMIZED VSP DETERMINATION

SITE LATITUDE = 36 DEGREES 5 MINUTES 3.78867 SECONDS
SITE LONGITUDE = -115 DEGREES 9 MINUTES 29.4578 SECONDS

1.2 optimum tilt angle in degrees

```

vsp 1501      82.0 - low beam reference attenuation
vsp 1502      120 - low beam STC slope (0.1 db/octave)
vsp 1503      121 - low beam STC slope (0.1 db/octave)
vsp 1504      120 - low beam STC slope (0.1 db/octave)
vsp 1505      165 - low beam STC slope (0.1 db/octave)
vsp 1506      42 - low beam STC slope (0.1 db/octave)
vsp 1507      1 - low beam STC slope (0.1 db/octave)
vsp 1508      22 - low beam STC slope (0.1 db/octave)
vsp 1509      0 - low beam STC slope (0.1 db/octave)
vsp 1601      76.0 - high beam reference attenuation
vsp 1602      120 - high beam STC slope (0.1 db/octave)
vsp 1603      135 - high beam STC slope (0.1 db/octave)
vsp 1604      124 - high beam STC slope (0.1 db/octave)
vsp 1605      149 - high beam STC slope (0.1 db/octave)
vsp 1606      6 - high beam STC slope (0.1 db/octave)
vsp 1607      0 - high beam STC slope (0.1 db/octave)
vsp 1608      0 - high beam STC slope (0.1 db/octave)
vsp 1609      0 - high beam STC slope (0.1 db/octave)

8 # of inner regions
vsp 1101      64 - start az adjct window (cpis)
vsp 1102      96 - start az adjct window (cpis)
vsp 1103      128 - start az adjct window (cpis)
vsp 1104      160 - start az adjct window (cpis)
vsp 1105      191 - start az adjct window (cpis)
vsp 1106      195 - start az adjct window (cpis)
vsp 1107      209 - start az adjct window (cpis)
vsp 1108      217 - start az adjct window (cpis)
vsp 1109      15 - range for adjct window (nmi)
vsp 1110      15 - range for adjct window (nmi)
vsp 1111      15 - range for adjct window (nmi)
vsp 1112      15 - range for adjct window (nmi)
vsp 1113      17 - range for adjct window (nmi)
vsp 1114      15 - range for adjct window (nmi)
vsp 1115      17 - range for adjct window (nmi)
vsp 1116      15 - range for adjct window (nmi)

2 # of is regions
isolated window # 1
vsp 1201      215 - start az isolated beam (cpis)
vsp 1202      4 - az extent isolated beam (cpis)
vsp 1203      24 - start range (nmi)
vsp 1204      25 - stop range (nmi)
vsp 1205      - high beam window

isolated window # 2
vsp 1206      203 - start az isolated beam (cpis)
vsp 1207      3 - az extent isolated beam (cpis)
vsp 1208      18 - start range (nmi)
vsp 1209      20 - stop range (nmi)
vsp 1210      - high beam window

```

matically select the best sites for sensor placements, based on operator-selected geographical constraints. Measures-of-merit for site placement will include the visibility of operator selected vectoring points, the runway visibility, the visibility of potential multipath regions, the visibility and orientation of highways, and the total volumetric coverage.

V. SUMMARY

In its current stage of development, the RSS provides a powerful tool for predicting the site-specific performance of PSR and SSR systems. By automating the site selection process, the RSS will help to significantly reduce the time required and the cost of sensor siting, while affording the siting engineer the opportunity to evaluate more than the handful of sites currently investigated when a new sensor location is to be chosen. Future RSS enhancements will provide this same benefit for other equipment, and will help to bring about an even higher level of siting automation.